Dalton Transactions

Accepted Manuscript

ROYAL SOCIETY OF CHEMISTRY

www.rsc.org/dalton

Cite this: DOI: 10.1039/c0xx00000x

www.rsc.org/xxxxxx

ARTICLE TYPE

Highly Efficient Electrochemiluminescence from Iridium(III) Complexes with 2-Phenylquinoline Ligand

Yuyang Zhou [*a], Wanfei Li [b], Linpo Yu [b], Yang Liu [b,c], Xiaomei Wang [a], Ming Zhou [*b,c]

Received (in XXX, XXX) Xth XXXXXXXXX 20XX, Accepted Xth XXXXXXXXX 20XX

DOI: 10.1039/b000000x

A series of cyclometalated iridium(III) complexes with 2-phenylquinoline ligand (**1**-**4**) were designed and synthesized, which were thoroughly investigated by the photophysics, electrochemistry, theoretical calculations and electrochemiluminescence (ECL). Through incorporating methyl groups into the 2-phenylquinoline, the corresponding complexes **2** and **3** displayed lower oxidative potential and higher HOMO energy level. Most importantly, compared with tris(2,2'-bipyridyl)ruthenium(II) ($[Ru(bipy)_3]^{2+}$), these iridium(III) complexes demonstrated more intense ECL in acetonitrile solutions.

Introduction

Since the first report on the electrochemiluminescence (ECL) behavior of tris(2,2'-bipyridyl)ruthenium(II) ($[Ru(bipy_{)3}]^{2+}$) by Bard et al. in the early 1970s,[1] the ECL phenomenon has been developed into a mature technology, specifically for immunoassay. As a well-studied luminescent metal complex, $[Ru(bipy)_3]^{2+}$ has been a key player for more than forty years in the ECL related scientific research and technological development.[2-4] Although other metal complexes such as europium,[5] rhenium,[6] copper,[7] osmium,[8] aluminum,[9, 10] terbium,[11] platinum,[12] iridium[12-19] have also been tested as ECL luminophores, none of them have received the same level of attention as we paid to $[Ru(bipy)_3]^{2+}$ and its analogues. However, a rising star from non-ruthenium systems seems to be cyclometalated iridium(III) complexes, because a number of promising results have been reported by the groups of Kapturkiewicz,[14, 20, 21] Richter,[13, 15] Kim[16, 22] and Ding[23, 24] et al.. Unlike ruthenium(II) polydiimine complexes, tris- or bis-cyclometalated iridium(III) complexes demonstrate a capability of emitting lights in a much broader spectral range (from NIR[25, 26] to blue[27, 28]). Another reason for the growing attention paid to cyclometalated iridium(III) is that a great number of iridium(III) complexes have been synthesized and well-studied for the organic light emitting diodes (OLEDs). The knowledge gained from the OLED research and the availability of various ligands help cyclometalated iridium(III) complexes becoming increasingly an ECL subject in the past few years.[23, 24, 29-34]

After reviewing a number of iridium(III) ECL luminophores, we were impressed by the result obtained by Kim et al.[16] from two ECL luminophores $(pq)_2Ir(acac)$ (**1** in Scheme 1) and $(pq)_2Ir(tmd)$ (pq, acac and tmd represent 2-phenylquinoline, 2,2',6,6'-tetramethylhepta-3,5-dione anion and dibenzoylmethane anion respectively). They were found to be 77- and 49-times more emissive than $Ru(bipy)_3^{2+}$,[16] respectively. In their follow-up work, by changing the ancillary ligands, Kim et al. further studied the ECL properties of a number of $(pq)_2Ir(LX)$ (LX was 3-isoquinaldate, picolinate anion, quinaldate anion), but the performance of luminophores $(pq)_2Ir(LX)$ with tripropylamine (TPA) is worse than the formerly reported luminophore $(pq)_2Ir(acac)$ (**1** in scheme 1).[22]

These $(pq)_2Ir(LX)$ complexes all have emission centered at about 600 nm, close to the emission of $[Ru(bipy)_3]^{2+}$. Such ECL luminophores, if applicable to the practical analytical assays, would not need a change of detector equipped in the current ECL measurement systems. Therefore, based on the previous results, we wish to further explore $(pq)_2Ir(acac)$ type compounds with focus on the derivatization of 2-phenylquinoline. In our search for better ECL luminophores, we realized that the TPA involved ECL process is rather complicated and the final ECL emission is a result of a cascade of electrochemical and follow-up chemical reactions. Any change of the ligands may have influence on the photophysical and electrochemical properties and the chemical reactivity towards other reactants, and eventually, lead to different ECL emission.

As illustrated in Scheme 1, a series of iridium(III) complexes

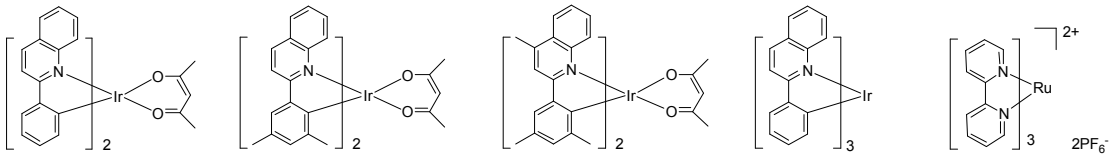

1 **2** **3** **4** **Ru(bipy)$_3$(PF$_6$)$_2$**

Scheme 1. Chemical structures of metal complexes used in this work.

(including a homoleptic complex) with at least two pq or methyl substituted pq were designed and synthesized. Their basic photophysical, electrochemical and ECL properties were reported below.

Results and discussion

Synthesis. The bis-heteroleptic iridium(III) complexes **1**, **2** and **3** were successfully synthesized through chloride-bridged dimers.[35] The homoleptic complex **4** was synthesized in a one-pot approach using $Ir(acac)_3$ as the starting material.[36] These methods have been well-established and there is no need to discuss further. Detailed analytical data were provided in Experimental Section.

Crystal structure of complex 1. Single crystal of complex **1** was grown from acetonitrile/methanol solution and characterized using X-ray crystallography. The molecular structure of **1** and the selected bond distances and angles are illustrated in Figure 1 and Table 1 & 2. As shown in Figure 1, two coordinated carbon atoms (C11 and C26, red in Figure 1) are in the *cis* position, while nitrogen atoms (N2 and N1, blue in Figure 1) of two cyclometalated ligands are in *trans* position. Table 2 demonstrates that the bond distances between coordinated atoms of the ancillary ligand and iridium(III) atom (Ir1-O1 and Ir1-O2) are slightly longer than those of the main ligand (Ir1-C11, Ir1-C26, Ir1-N1 and Ir1-N2). Accordingly, the bite angle of ancillary ligand (O1-Ir1-O2) is also a little larger than those of main ligands (C26-Ir1-N2 and C11-Ir1-N1). The detailed crystallographic data are listed in Table 1.

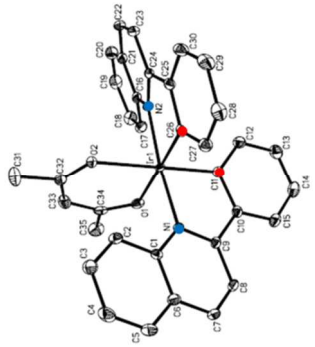

Figure 1. Crystal structure of complex **1**. The hydrogen atom was omitted for clarity.

Table 1. X-ray crystallographic data for complex **1**

Empirical formula	$C_{35}H_{27}IrN_2O_2(CH_3CN)$
Formula weight	740.84
Temperature	153(2)
Wavelength(Å)	0.71073
Crystal system	Monoclinic
Space group	P 21/c
a (Å)	9.6878(4)
b (Å)	17.3589(7)
c (Å)	17.8512(8)
α (deg)	90
β (deg)	101.5150(11)
γ (deg)	90
Volume ($Å^3$)	2941.6(2)
Z	4
$D_{calcd}(mg/m^3)$	1.673
Absorption coefficient(mm^{-1})	4.578
F(000)	1464
Crystal size (mm)	0.48×0.46×0.30
$2\theta_{max}$ (deg)	52.74
Goodness-of-fit on F^2	1.072
Final R indices [I>2σ(I)]	0.0169
R1(all data)	0.0186
wR2(all data)	0.0420

Table 2. Selected bond lengths (Å) and angles (deg) for complex **1**

Selected bond lengths (Å)	
Ir(1)-C(11)	1.978(2)
Ir(1)-C(26)	1.986(2)
Ir(1)-N(2)	2.0811(18)
Ir(1)-N(1)	2.0856(17)
Ir(1)-O(1)	2.1572(15)
Ir(1)-O(2)	2.1620(14)
Selected angles (deg)	
C(26)-Ir(1)-N(2)	80.33(8)
C(11)-Ir(1)-N(1)	80.56(8)
O(1)-Ir(1)-O(2)	86.70(6)
C(11)-Ir(1)-C(26)	92.83(8)
C(11)-Ir(1)-N(2)	96.16(8)

Theoretical calculations. In order to further investigate the properties of these novel complexes in this work, DFT and TD-DFT calculations were also carried out to investigate the ground and excited states of **1**-**4** by Gaussian 03 package. The 6-31G basis set was used for C, N, H, O and atom iridium employed the LANL2DZ basis set, which have been proved reliable for cyclometalated iridium(III) complexes.[37-39] The frontier orbitals involved the singlet and triplet electron distributions for **1**-**4** are shown in Table 3, while the calculated transition wavelength and assignment are listed in Table 4.

According to the Table 4, the singlet states of **1**-**4** are all mainly assigned to the HOMO→LUMO while the triplet states are much more complicated. The electron distributions of the HOMO are mainly located on the central Ir metal atom and phenyl group of the bidentate ligand (C^N), while those LUMO are mainly on quinoline group of bidentate ligand (C^N). Based on the electron distributions on the frontier orbital involved in the transition states as shown in Table 4, we reasonably presumed that the nature of the excited state of these complexes mainly consists of a mixture of ^{3}MLCT [$d\pi(Ir)\rightarrow\pi^*_{C^N}$] and ^{3}ILCT [$\pi_{phenyl}\rightarrow\pi^*_{quinoline}$].

The ECL emission involved redox process of the luminophore and co-reactant, so the HOMO and LUMO energy of both the neutral and mono-cationic form of **1**-**4** were also calculated and listed in Table 5. The calculation results indicated that for both the neutral and mono-cationic form, the methyl group would increase the HOMO and LUMO energies of the corresponding complex. According to the literatures,[40, 41] the luminophore with the lower LUMO energy level of the mono-cationic form is usually expected to have a higher ECL intensity. In this work, the LUMO energy levels both forms follow the same sequence: complex **1** < complex **2** < complex **4** < complex **3**. However, the following ECL experiment results (see Table 8) showed that the complex **2** and **3**, not complex **1**, displayed the highest ECL intensity, indicating that the ECL process is complicated and the ECL intensity is hardly a function of a single parameter.

Table 3. Frontier orbitals of **1-4** obtained for the optimized structures of the ground state.

Complex	HOMO-2	HOMO	LUMO	LUMO+1
1	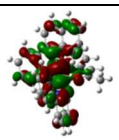	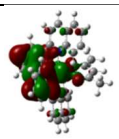	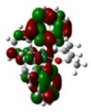	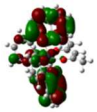
2	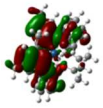	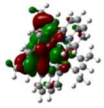	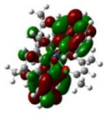	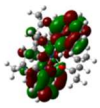
3	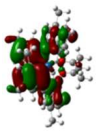	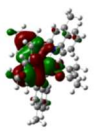	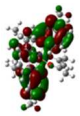	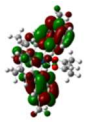
4	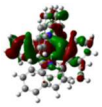	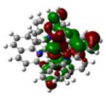	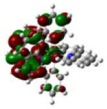	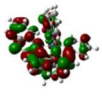

Table 4. Calculated transition wavelength, oscillator strength (*f*) and molecular orbitals involved in the lowest-energy transition of **1-4**.

Complex	State	λ_{max} [nm]	*f*	Assignments
1	T_1	574.30	0.0000	HOMO→LUMO (67.79%) HOMO-3→LUMO+1 (16.70%) HOMO-2→LUMO (+12.12%)
	S_1	532.02	0.0023	HOMO→LUMO (68.37%)
2	T_1	612.21	0.0000	HOMO→LUMO (69.48%) HOMO-2→LUMO+1 (13.74%)
	S_1	564.52	0.0024	HOMO→LUMO (68.66%)
3	T_1	603.07	0.0000	HOMO→LUMO (69.41%) HOMO-2→LUMO+1 (+14.01%)
	S_1	557.58	0.0027	HOMO→LUMO (68.68%)
4	T_1	573.23	0.0000	HOMO→LUMO (66.10%) HOMO-2→LUMO (+12.66%) HOMO→LUMO+1 (+11.39%)
	S_1	545.61	0.0160	HOMO→LUMO (68.40%)

Table 5. The HOMO and LUMO energy of the neutral and momo-cationic form of **1-4**.

Complex	Neutral form		Mono-cationic form	
	HOMO(eV)	LUMO(eV)	HOMO(eV)	LUMO(eV)
1	-4.76	-1.78	-8.57	-4.79
2	-4.60	-1.76	-8.27	-4.69
3	-4.53	-1.67	-8.17	-4.55
4	-4.71	-1.75	-8.00	-4.67

Absorption and photoluminescence. The electronic absorption spectra of **1-4** in acetonitrile solutions are presented in Figure 2A. Since $Ru(bipy)_3(PF_6)_2$ is used as the reference for ECL, its absorption spectrum is also shown in Figure 2A.

Like other iridium(III) complexes reported before,[42-48] **1-4** in this work also have strong intraligand absorption bands (π–π*) in UV region (below 300 nm, ε >10000 M^{-1} cm^{-1}) and a broad

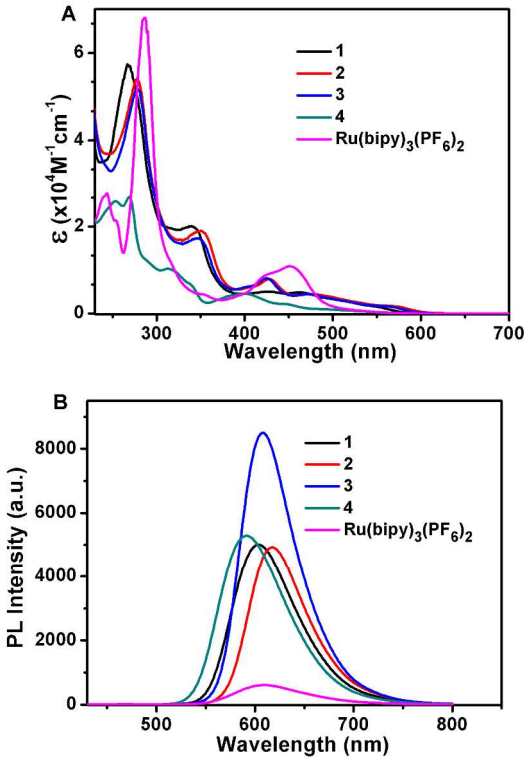

Figure 2. Absorption (A) and photoluminescence (B) spectra of **1-4** in deaerated acetonitrile solutions. The concentrations were 40 μM and 10 μM for absorption and photoluminescence, respectively. λ_{ex} = 410 nm.

Table 6. Spectroscopic data of **1-4** in acetonitrile solutions.

Complex	Absorption, ε (10^4 $M^{-1}cm^{-1}$)		Emission (410 nm excitation)			
	max@ λ (nm)	@ 410 nm	λ_{max} (nm)	I_s / I_{ref}	A_s / A_{ref}	Φ_{PL}
1	0.48@462; 0.50@427 2.00@340; 5.74@267	0.47	604	7.41	0.76	0.60
2	0.45@474; 0.79@428 1.90@350; 5.42@278	0.62	618	6.71	1.00	0.42
3	0.44@469; 0.81@425 1.73@347; 5.17@279	0.65	608	11.13	1.05	0.66
4	0.46@399; 1.03@312 2.68@269; 2.58@254	0.41	591	8.12	0.66	0.76
$Ru(bipy)_3(PF_6)_2$	1.09@451; 0.85@421 6.80@287; 2.76@244	0.62	609	1	1	0.062*

* see ref. 49

featureless MLCT (d-π*) transition in the visible light (400-600 nm, ε<8000 M^{-1} cm^{-1}). Compared with the intense MLCT band of $Ru(bipy)_3(PF_6)_2$, **1-4** show weaker absorption band between 400-500 nm. There are no obvious visible absorption bands beyond 600 nm for all these iridium(III) complexes.

In order to measure the photoluminescence (PL) quantum efficiency (Φ_{PL}), we chose $Ru(bipy)_3(PF_6)_2$ as the reference, under the excitation of 410 nm light. The selection of 410 nm is a compromise that enabled both the iridium(III) luminophores and $Ru(bipy)_3(PF_6)_2$ to be compared under the condition that all compounds have absorption close to each other. The photoluminescent spectra of **1-4** and $Ru(bipy)_3(PF_6)_2$ used in this work are shown in Figure 2B.

The emission wavelength of these iridium(III) complexes are

centered in a narrow range of 591 ~ 618 nm, close to that of $Ru(bipy)_3(PF_6)_2$, while the luminescence intensity have a great variation. Numerical comparison is presented in Table 6. It demonstrated that two methyl substituents on the phenyl group of main ligand induced a 14 nm red shift of the PL peak wavelength of complex **2** relative to complex **1**. However, further incorporating one methyl substituent into the quinoline group of the main ligand, a blue shift of 10 nm is observed from complex **2** to complex **3**. In addition, a blue shift of PL peak wavelength from 604 nm of the heteroleptic complex **1** to 591 nm of the correspondingly homoleptic complex **4** was also found. The emission intensity (*I*) was taken as the integration of the emission spectra from 450 to 800 nm. Based on the excitation coefficients at 410 nm and the emission intensities, the photoluminescence quantum efficiencies of the iridium(III) complexes were calculated by using $Ru(bipy)_3(PF_6)_2$ as the standard (0.062, in acetonitrile[49]). Just as many other iridium(III) complexes reported before[36, 50], **1**-**4** in this work have higher photoluminescence quantum efficiencies than that of the reference $Ru(bipy)_3(PF_6)_2$. Moreover, though the skeleton of these iridium complexes were similar, the photoluminescent quantum efficiencies were variable due to the methyl substituent and coordination mode.

Electrochemistry. Before the ECL study, we further conducted electrochemical characterization of complexes **1**-**4** by cyclic voltammetry (CV) in order to gain the redox properties of these cyclometalated iridium(III). Cyclic voltammograms of **1**-**4** obtained at a platinum electrode are shown in Figure 3 and the numerical comparison is summarized in Table 7.

According to Figure 3 and Table 7, at the scan rate of 100 mV s^{-1}, complexes **1**-**4** demonstrated a reversible oxidation wave at the potential range between 0.34~0.53 V and a reversible reduction wave at the potential range between -2.23~ -2.31 V. Comparing the E_a^{ox} of **1**, **2** and **3**, we found that the substituent of $–CH_3$ on the 2-phenylquinoline ligand brings the oxidative potential down. On the other hand, the $–CH_3$ substitution doesn't have significant effects on reductive potential.

Electrochemiluminescence (ECL). The oxidative-reduction ECL of **1**-**4** was generated by both potential scanning and potential stepping technique in TPA-containing acetonitrile solutions.

In the potential scanning experiments (Figure 4), the reversible oxidation wave of iridium(III) complexes were hidden by the strong irreversible TPA oxidation wave due to the much higher concentration of TPA. For **2** and **3**, the ECL started to show up at the same time when TPA was oxidized. However, for their higher oxidation potentials, the ECL of **1** and **4** lagged behind the TPA oxidation.

The ECL intensities were measured by integrating the PMT signal from 0.4 V to 1.2 V during the forward scans. Taking $Ru(bipy)_3(PF_6)_2$ as a reference (ECL intensity 1), the ECL intensities of **1**-**4** were listed in Table 8. As can be seen from the Table 8, **2** outperformed all other luminophores and showed an ECL intensity that was 230 times higher than that of $Ru(bipy)_3(PF_6)_2$.

The ECL intensities were also compared in the potential stepping experiments (Figure 5). The applied potential was 1.2 V (*vs* Fc/Fc^+) and the ECL was recorded as a function of time. For a comparison, the ECL intensities were measured arbitrarily as the integration of the PMT signal over the period of 0-2 second. The

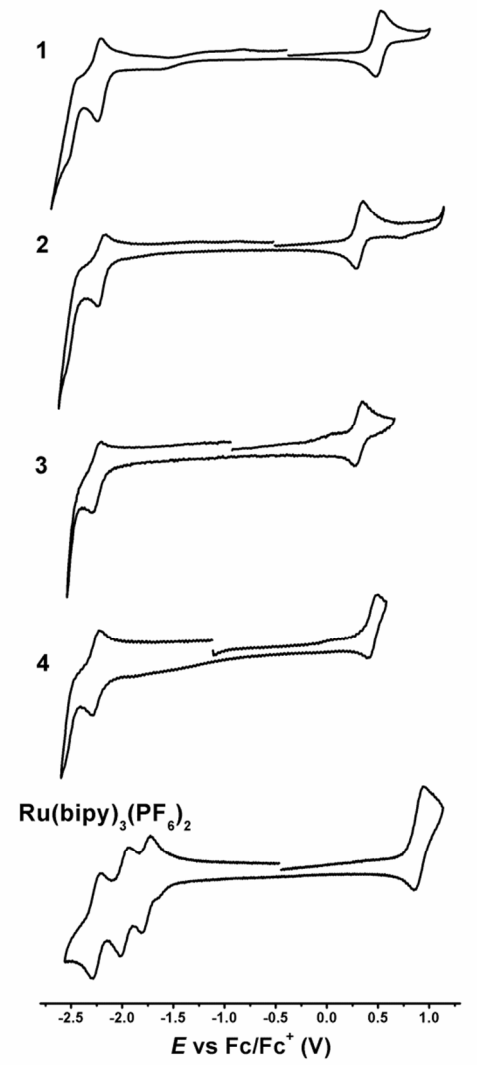

Figure 3. Cyclic voltammograms of 0.5 mM **1**-**4** and $Ru(bipy)_3(PF_6)_2$ with 0.1 M $TBAPF_6$ (**4** in DMF solution due to its low solubility and others in acetonitrile solutions). Pt electrode area 0.785 mm^2, scan rate: 100 mV/s.

Table 7. Electrochemical data and energy levels of **1**-**4**.[a]

Complex	E_a^{ox}(V)	E_{onset}^{ox} (V)	E_c^{re}(V)	E_{onset}^{re}(V)
1	0.53	0.42	-2.24	-2.11
2	0.35	0.23	-2.23	-2.12
3	0.34	0.18	-2.28	-2.12
4	0.48	0.34	-2.31	-2.05
$Ru(bipy)_3(PF_6)_2$	0.95	0.77	-1.80, -2.01, -2.28	-1.62

[a] All the electrochemical potentials were calibrated with ferrocene/ferrocenium (Fc/Fc^+) redox couple.

relative ECL intensities were also listed in Table 8.

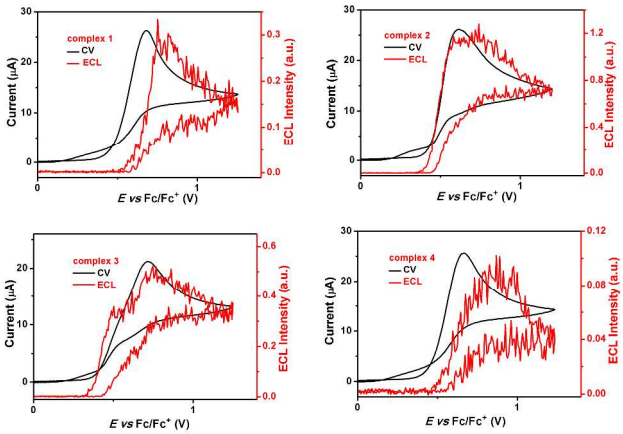

Figure 4. Cyclic voltammograms and ECL intensity *vs* potential plots of 0.1 mM **1**-**4** in acetonitrile with 0.1 M $TBAPF_6$ and 0.01 M TPA.

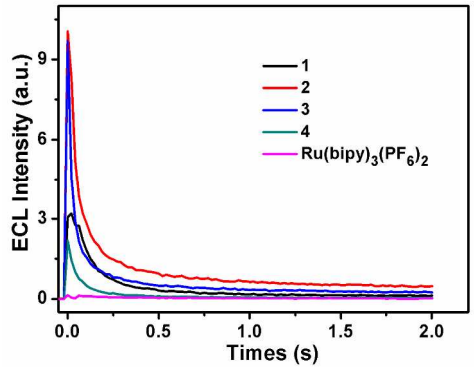

Figure 5. ECL intensity *vs* time plot of 0.1 mM **1**-**4** and $Ru(bipy)_3(PF_6)_2$ with 0.1 M $TBAPF_6$ and 0.01 M TPA in acetonitrile. Potential step at 1.2 V (*vs*. Fc/Fc^+).

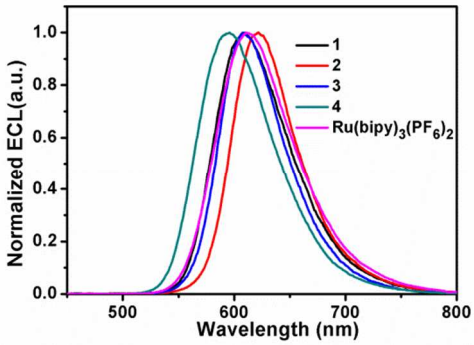

Figure 6. Normalized ECL spectra of 0.1 mM **1**-**4** and $Ru(bipy)_3(PF_6)_2$ with 0.1 M $TBAPF_6$ and 0.01 M TPA in acetonitrile. Potential step at 1.2 V (*vs*. Fc/Fc^+). The spectra were collected after the potential pulse was employed and the ECL intensity decayed to a plateau stage.

In addition to the above oxidative-reduction ECL processes, we also carried out the annihilation experiments, in which both the oxidized iridium complexes and the reduced iridium complexes were alternatively generated on the electrode at the potentials of E_a^{ox}+0.2 and E_c^{re}-0.2 in anhydrous acetonitrile solutions. The typical ECL generated by this approach is displayed in Figure S16 (see Supporting Information). The ECL was recorded as the integration over a certain period of time and compared with that of $Ru(bipy)_3(PF_6)_2$. The mechanism of ECL from annihilation process can be similarly illustrated on the basis of the extensively studied $Ru(bipy)_3(PF_6)_2$ system[51-53] and other iridium(III) complex/TPA system.[22, 54]

Table 8. Electrochemiluminescene data of **1**-**4** and $Ru(bipy)_3(PF_6)_2$ in this work.[a]

Complex	Wavelength (nm)	I_s/I_{ref} [b]	I_s/I_{ref} [c]	I_s/I_{ref} [d]
1	610	42.50	10.26	1.31
2	622	234.65	37.62	71.62
3	608	108.49	20.80	177.00
4	596	14.18	2.73	3.42
$Ru(bipy)_3(PF_6)_2$	611	1.00	1.00	1.00

[a] acetonitrile solution of 0.1 M TBAPF6. [b] Potential scanning experiment, 100 mV/s, 0.1 mM complex/0.01 M TPA system. [c] Potential stepping experiment, at 1.2 V vs Fc/Fc^+, 2 s acquisition, 0.1 mM complex/0.01 M TPA system. [d] Annihilation experiment, oxidative potential at E_a^{ox}+0.2 V, reductive potential at E_c^{re}-0.2 V, 0.1 mM complex, 10 Hz, 20 s acquisition). I_s and I_{ref} denote the integration of the ECL signals of iridium complexes and the reference $Ru(bipy)_3(PF_6)_2$, respectively.

An ECL efficiency has been sometimes used in ECL research. The concept of ECL efficiency in the annihilation is well defined and makes sense. But it can hardly be established in the oxidative-reduction and reductive-oxidation mechanisms, because of the complicated ECL generation processes either by potential scanning or by potential stepping. Thus, we compare the ECL intensities of the iridium(III) complexes relative to $Ru(bipy)_3(PF_6)_2$. The numerical results extracted from the ECL experiments are summarized in Table 8.

The ECL spectra were collected when the ECL intensity decayed to a plateau stage.[31] According to Figure 6 and the numerical data listed in Table 8, all these complexes have ECL emission centered at a narrow range between 596 nm to 622 nm, which is close to 611 nm of $Ru(bipy)_3(PF_6)_2$. The maximum wavelengths of the ECL are, within the experimental errors, the same as those of PL, indicating the same excited states that are responsible for the emission.

In summary, it is confirmed that compound **1**, as it was first demonstrated in Kim and co-workers' work, is an ECL luminophore with stronger ECL emission than that of $Ru(bipy)_3(PF_6)_2$. Furthermore, by introducing methyl groups to the cyclometalated ligands, the compounds, such as **2** and **3**, demonstrated even higher ECL emission in acetonitrile solutions. It should be noted that, when using the TPA as the co-reactant, the ECL intensity of complex **2** outperformed that of complex **3**, however, complex **3** displayed higher ECL intensity under the annihilation process.

Conclusion

In this work, through decorating the main ligand and changing the coordination mode, a series of cyclometalated iridium(III) complexes with 2-phenylquinoline or its derivatives (**1-4**) were designed, synthesized and characterized by photophysics, electrochemistry and ECL. The comparative ECL studies in acetonitrile solutions shows that the new luminophore of **2** and **3** with methyl substituents on the main ligands demonstrated ECL emission much stronger than that of $Ru(bipy)_3(PF_6)_2$ and that of luminophore **1**. These results are useful for further development novel ECL luminophores and ECL labels for analytical applications.

Experiment Section

Chemicals. 2-phenylquinoline, 2-(3,5-dimethylphenyl)quinoline and 2-(3,5-dimethylphenyl)-4-methylquinoline and the standard luminophore of $Ru(bipy)_3(PF_6)_2$ were all received from SunaTech Inc., while acetylacetone were purchased from Sinopharm Chemical Reagent Co., Ltd. Acetonitrile (Spectrophotometric grade, Sinopharm Chemical Reagent Co. Ltd.) was used for photophysics studies, while anhydrous acetonitrile (99.9%, Acros), tetra-*n*-butylammonium hexafluorophosphate ($TBAPF_6$, electrochemical grade, Fluka) and tri-*n*-propylamine (TPA) were used for electrochemical characterization as received. Complexes **1-4** were synthesized and purified according to the literature.[36]

Molecular structure characterization.

Complex **1** (Yield: 78%, UPLC purity: 98%). ^{1}H NMR (DMSO-d_6, 400 MHz). δppm: 1.46 (s, 6 H), 4.70 (s, 1 H), 6.30 (d, J=8 Hz, 2 H), 6.54 (t, J=8 Hz, 2 H), 6.89 (t, J=8 Hz, 2 H), 7.56 (m, 4 H), 8.01 (m, 4 H), 8.40 (m, 4 H), 8.50 (d, J=8 Hz, 2 H). ^{13}C NMR (DMSO-d_6, 100 MHz). δppm: 185.56, 170.37, 150.47, 148.96, 147.64, 139.41, 135.72, 130.98, 128.78, 127.50, 126.79, 126.58, 126.09, 121.18, 117.50, 100.73, 28.43. Tof-mass: calculated $[M+Na]^+$ 721.1571, observed $[M+Na]^+$ 721.1578.

Complex **2** (Yield: 72%, UPLC purity: 98%). ^{1}H NMR (DMSO-d_6, 400 MHz). δppm: 1.12 (s, 6 H), 1.27 (s, 6 H), 2.30 (s, 6 H), 4.30 (s, 1 H), 6.43 (s, 2 H), 7.38-7.50 (m, 4 H), 7.76 (m, 4 H), 7.90 (d, J=8 Hz, 2 H), 8.35 (m, 4 H). ^{13}C NMR (DMSO-d_6, 100 MHz). δppm: 184.26,169.79, 148.81, 148.68, 147.03, 145.97, 138.11, 130.52, 130.12, 130.00, 128.48, 126.07, 125.39, 125.23, 118.08, 99.43, 28.05, 22.92, 21.11. Tof-mass: calculated $[M+Na]^+$ 777.2197, observed $[M+Na]^+$ 777.2182.

Complex **3** (Yield: 64%, UPLC purity: 98%). ^{1}H NMR (DMSO-d_6, 400 MHz). δppm: 1.10(s, 6 H), 1.27 (s, 6 H), 2.30 (s, 6 H), 2.85 (s, 6 H), 4.32 (s, 1 H), 6.40 (s, 2 H), 7.40 (t, J=8 Hz, 2 H), 7.49 (t, J=8 Hz, 2 H), 7.75 (s, 2 H), 7.81 (d, J=8 Hz, 2 H), 8.22 (s, 1 H). ^{13}C NMR (CD_2Cl_2, 100 MHz). δppm: 184.40, 169.00, 148.44, 148.39, 146.62, 146.18, 145.33, 130.38, 130.09, 129.35, 126.08, 125.98, 125.16, 124.26, 123.80, 118.11, 98.56, 27.55, 22.53, 20.67, 19.02. Tof-mass: calculated $[M+Na]^+$ 805.2510, observed $[M+Na]^+$ 805.2529.

Complex **4** (Yield: 58%, UPLC purity: 98%). ^{1}H NMR (DMSO-d_6, 400 MHz). δppm: 6.29 (d, J=8 Hz, 1 H), 6.57 (t, J=8 Hz, 1 H), 6.70 (m, 1 H), 6.80 (m, 1 H), 7.30 (t, J= 8 Hz, 1 H), 7.90 (m, 3 H), 8.38 (m, 2 H). ^{13}C NMR (DMSO-d_6, 100 MHz). Tof-Mass: calculated $[M+Na]^+$ 805.2510, observed $[M+Na]^+$ 805.2529. Tof-mass: calculated $[M+Na]^+$ 826.1938, observed $[M+Na]^+$ 826.1933.

X-ray structure determination. A suitable crystal of complex **3** was mounted on a glass fiber and transferred to a Rigaku Mercury CCD area detector at 293 K. The structure was resolved and refined by full-matrix least-squares procedures based on F^2 using SHELXS-97 and SHELXL-97 programs, respectively. All non-hydrogen atoms were refined anisotropically, while hydrogen atoms were treated as idealized contributions.

Measurements. The UV-Vis absorption spectra and emission spectra were obtained on a Perkin Elmer Lambda 25 UV-Vis spectrophotometer and a HITACHI F-4600 spectrofluorophotometer, respectively. Both absorption and emission measurements were carried out in deaerated acetonitrile. The photoluminescence quantum yields (Φ_{PL}) were calculated according to the equation: $\Phi_{PL} = \Phi_{ref}(I_s/I_{ref})(A_{ref}/A_s)$, in which A is the absorbance at the excitation wavelength, I is the integrated intensity of the luminescence, Φ is the photoluminescence quantum efficiency, the subscripts *s* and *ref* refer to the sample and standard, respectively. An acetonitrile solution of $Ru(bipy)_3(PF_6)_2$ was used as a standard with Φ_{PL}=0.062.[49]

A home-built measurement setup was used for both electrochemical and electrochemiluminescence studies. A PARSTAT 2263-2 Advanced Electrochemical System with Powersuit software was used for electrochemical measurement. Cyclic voltammetry measurement was performed in a three-electrode configuration using a Pt disk (diameter 1 mm, area 0.785 mm^2) sealed in a PTFE rod as the working electrode. Prior to each electrochemical experiment, it was polished with alumina polishing paste (diameter 0.25 μm), rinsed thoroughly with water and acetone, and dried by a warm air flow. Both the counter and quasi-reference electrodes are Pt wires. The cyclic voltammetry measurement and ECL studies used the same electrochemical cell. All the potentials were calibrated with ferrocene/ferrocenium (Fc/Fc^+) redox couple as a reference.

Acknowledgment

The authors are grateful to the Opening Project (No.SJHG1305) of the Jiangsu Key Laboratory for Environment Functional Materials, Natural Science Foundation of Jiangsu Province (Grant No. BK20131152), the Excellent Innovation Team in Science and Technology of University in Jiangsu Province, University Scientific Research Project of Jiangsu Province (11KJB430012), the Scientific Research Foundation of the Chinese Ministry of Education ([2013]693) and the National Natural Science Foundation of China (Grant No. 21107077, 21103119, 21005084) for the financial support.

Notes and references

[a] *Jiangsu Key Laboratory of Environmental Functional Materials, School of Chemistry, Biology and Material Engineering, Suzhou University of Science and Technology, Suzhou, Jiangsu, 215009, P. R.China. E-mail:zhouyuyang@mail.usts.edu.cn.*

[b] *Division of Nanobiomedicine, Suzhou Institute of Nano-Tech and Nano-Bionics, Chinese Academy of Sciences, 398 Ruoshui Road, Suzhou Industrial Park, Suzhou, Jiangsu, 215123, P. R. China. Fax: +86-512-62872553. E-mail: mzhou2007@sinano.ac.cn.*

[c] *SunaTech Inc., bioBAY, Suzhou Industrial Park, Suzhou, Jiangsu, 215123, P. R. China.*

† Electronic Supplementary Information (ESI) available: ^{1}H NMR, ^{13}C NMR, tof-mass and UPLC charactizations; the ECL intensity vs time plot generated by annihilation process about complex **3**. See DOI: 10.1039/b000000x/.

1. N. E. Tokel and A. J. Bard, *J. Am. Chem. Soc.*, 1972, **94**, 2862-2863.
2. M. M. Richter, *Chem. Rev.*, 2004, **104**, 3003-3036.
3. H. Wei and E. Wang, *Luminescence*, 2011, **26**, 77-85.
4. L. Hu and G. Xu, *Chem. Soc. Rev.*, 2010, **39**, 3275-3304.
5. M. M. Richter and A. J. Bard, *Anal. Chem.*, 1996, **68**, 2641-2650.
6. M. M. Richter, J. D. Debad, D. R. Striplin, G. A. Crosby and A. J. Bard, *Anal. Chem.*, 1996, **68**, 4370-4376.
7. J. McCall, D. Bruce, S. Workman, C. Cole and M. M. Richter, *Anal. Chem.*, 2001, **73**, 4617-4620.
8. D. Bruce, M. M. Richter and K. J. Brewer, *Anal. Chem.*, 2002, **74**, 3157-3159.
9. J. D. Anderson, E. M. McDonald, P. A. Lee, M. L. Anderson, E. L. Ritchie, H. K. Hall, T. Hopkins, E. A. Mash, J. Wang, A. Padias, S. Thayumanavan, S. Barlow, S. R. Marder, G. E. Jabbour, S. Shaheen, B. Kippelen, N. Peyghambarian, R. M. Wightman and N. R. Armstrong, *J. Am. Chem. Soc.*, 1998, **120**, 9646-9655.
10. E. M. Gross, J. D. Anderson, A. F. Slaterbeck, S. Thayumanavan, S. Barlow, Y. Zhang, S. R. Marder, H. K. Hall, M. F. Nabor, J. F. Wang, E. A. Mash, N. R. Armstrong and R. M. Wightman, *J. Am. Chem. Soc.*, 2000, **122**, 4972-4979.
11. S. Kulmala, M. Håkansson, A. M. Spehar, A. Nyman, J. Kankare, K. Loikas, T. Ala-Kleme and J. Eskola, *Anal. Chim. Acta*, 2002, **458**, 271-280.
12. E. M. Gross, N. R. Armstrong and R. M. Wightman, *J. Electrochem. Soc.*, 2002, **149**, E137-E142.
13. D. Bruce and M. M. Richter, *Anal. Chem.*, 2002, **74**, 1340-1342.
14. A. Kapturkiewicz and G. Angulu, *Dalton Trans.*, 2003, 3907-3913.
15. B. D. Muegge and M. M. Richter, *Anal. Chem.*, 2004, **76**, 73-77.
16. J. I. Kim, I.-S. Shin, H. Kim and J.-K. Lee, *J. Am. Chem. Soc.*, 2005, **127**, 1614-1615.
17. M. J. Li, P. Jiao, M. Lin, W. He, G. N. Chen and X. Chen, *Analyst*, 2011, **136**, 205-210.
18. C. Li, J. Lin, Y. Guo and S. Zhang, *Chem. Commun.*, 2011, **47**, 4442-4444.
19. W. Yang, D. Wang, Q. Song, S. Zhang, Q. Wang and Y. Ding, *Organometallics*, 2013, **32**, 4130-4135.
20. A. Kapturkiewicz, T.-M. Chen, I. R. Laskar and J. Nowacki, *Electrochem. Commun.*, 2004, **6**, 827-831.
21. A. Kapturkiewicz, J. Nowacki and P. Borowicz, *Electrochim. Acta*, 2005, **50**, 3395-3400.
22. I.-S. Shin, J. I. Kim, T.-H. Kwon, J.-I. Hong, J.-K. Lee and H. Kim, *J. Phys. Chem. C*, 2007, **111**, 2280-2286.
23. K. N. Swanick, S. Ladouceur, E. Zysman-Colman and Z. Ding, *Chem. Commun.*, 2012, **48**, 3179-3181.
24. K. N. Swanick, S. Ladouceur, E. Zysman-Colman and Z. Ding, *RSC Advances*, 2013, **3**, 19961-19964.
25. S. Zhang, M. Hosaka, T. Yoshihara, K. Negishi, Y. Iida, S. Tobita and T. Takeuchi, *Cancer Res.*, 2010, **70**, 4490-4498.
26. Q. Zhang, R. Cao, H. Fei and M. Zhou, *Dalton Trans.*, 2014, DOI: 10.1039/C4DT00823E.
27. Y. Zhou, J. Jia, W. Li, H. Fei and M. Zhou, *Chem. Commun.*, 2013, **49**, 3230-3232.
28. Y. Zhou, W. Li, Y. Liu, L. Zeng, W. Su and M. Zhou, *Dalton Trans.*, 2012, **41**, 9373-9381.
29. K. N. Swanick, S. Ladouceur, E. Zysman-Colman and Z. Ding, *Angew. Chem. Int. Ed.*, 2012, **51**, 11079-11082.
30. U. M. Tefashe, K. L. Metera, H. F. Sleiman and J. Mauzeroll, *Langmuir*, 2013, **29**, 12866-12873.
31. L. Yu, Z. Huang, Y. Liu and M. Zhou, *J. Organomet. Chem.*, 2012, **718**, 14-21.
32. S. Zanarini, M. Felici, G. Valenti, M. Marcaccio, L. Prodi, S. Bonacchi, P. Contreras-Carballada, R. M. Williams, M. C. Feiters, R. J. M. Nolte, L. De Cola and F. Paolucci, *Chem. Eur. J.*, 2011, **17**, 4640-4647.
33. C. Li, J. Lin, Y. Guo and S. Zhang, *Chem. Commun.*, 2011, **47**, 4442-4444.
34. B. D. Stringer, L. M. Quan, P. J. Barnard, D. J. D. Wilson and C. F. Hogan, *Organometallics*, 2014, **33**, 4860-4872.
35. S. Lamansky, P. Djurovich, D. Murphy, F. Abdel-Razzaq, H.-E. Lee, C. Adachi, P. E. Burrows, S. R. Forrest and M. E. Thompson, *J. Am. Chem. Soc.*, 2001, **123**, 4304-4312.
36. S. Lamansky, P. Djurovich, D. Murphy, F. Abdel Razzaq, R. Kwong, I. Tsyba, M. Bortz, B. Mui, R. Bau and M. E. Thompson, *Inorg. Chem.*, 2001, **40**, 1704-1711.
37. L. Shi, J. Su and Z. Wu, *Inorg. Chem.*, 2011, **50**, 5477-5484.
38. L. Shi, B. Hong, W. Guan, Z. Wu and Z. Su, *J. Phys. Chem. A*, 2010, **114**, 6559-6564.
39. X. N. Li, Z. J. Wu, Z. J. Si, H. J. Zhang, L. Zhou and X. J. Liu, *Inorg. Chem.*, 2009, **48**, 7740-7749.
40. G. J. Barbante, E. H. Doeven, E. Kerr, T. U. Connell, P. S. Donnelly, J. M. White, T. Lópes, S. Laird, D. J. D. Wilson, P. J. Barnard, C. F. Hogan and P. S. Francis, *Chem. Eur. J.*, 2014, **20**, 3322-3332.
41. S. Zhu, Q. Song, S. Zhang and Y. Ding, *J. Mol. Struct.*, 2013, **1035**, 224-230.
42. Y. H. Song, Y. C. Chiu, Y. Chi, Y. M. Cheng, C. H. Lai, P. T. Chou, K. T. Wong, M. H. Tsai and C. C. Wu, *Chem. Eur. J.*, 2008, **14**, 5423-5434.
43. C. H. Hsieh, F. I. Wu, C. H. Fan, M. J. Huang, K. Y. Lu, P. Y. Chou, Y. H. Yang, S. H. Wu, I. C. Chen, S. H. Chou, K. T. Wong and C. H. Cheng, *Chem. Eur. J.*, 2011, **17**, 9180-9187.
44. C. J. Chang, C. H. Yang, K. Chen, Y. Chi, C. F. Shu, M. L. Ho, Y. S. Yeh and P. T. Chou, *Dalton Trans.*, 2007, 1881-1890.
45. J. Y. Hung, Y. Chi, I. H. Pai, Y. C. Yu, G. H. Lee, P. T. Chou, K. T. Wong, C. C. Chen and C.-C. Wu, *Dalton Trans.*, 2009, 6472-6475.
46. C. H. Lin, Y. Chi, M. W. Chung, Y. J. Chen, K. W. Wang, G. H. Lee, P. T. Chou, W. Y. Hung and H. C. Chiu, *Dalton Trans.*, 2011, **40**, 1132-1143.
47. J. Li, P. I. Djurovich, B. D. Alleyne, M. Yousufuddin, N. N. Ho, J. C. Thomas, J. C. Peters, R. Bau and M. E. Thompson, *Inorg. Chem.*, 2005, **44**, 1713-1727.
48. T. Sajoto, P. I. Djurovich, A. Tamayo, M. Yousufuddin, R. Bau, M. E. Thompson, R. J. Holmes and S. R. Forrest, *Inorg. Chem.*, 2005, **44**, 7992-8003.
49. J. V. Caspar and T. J. Meyer, *J. Am. Chem. Soc.*, 1983, **105**, 5583-5590.
50. C.-F. Chang, Y.-M. Cheng, Y. Chi, Y.-C. Chiu, C. C. Lin, G.-H. Lee, P.-T. Chou, C.-C. Chen, C.-H. Chang and C.-C. Wu, *Angew. Chem. Int. Ed.*, 2008, **47**, 4542-4545.
51. F. Kanoufi, Y. Zu and A. J. Bard, *J. Phys. Chem. B*, 2001, **105**, 210-216.
52. M. Zhou, G. P. Robertson and J. Roovers, *Inorg. Chem.*, 2005, **44**, 8317-8325.
53. W. Miao, J.-P. Choi and A. J. Bard, *J. Am. Chem. Soc.*, 2002, **124**, 14478-14485.
54. J. I. Kim, I.-S. Shin, H. Kim and J.-K. Lee, *J. Am. Chem. Soc.*, 2005, **127**, 1614-1615.

Highly Efficient Electrochemiluminescence from Iridium(III) Complexes with 2-Phenylquinoline Ligand

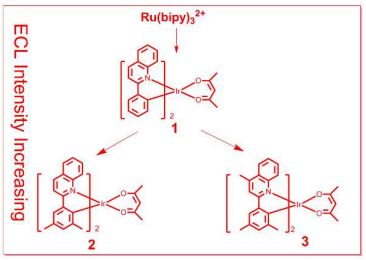

Bis-(methylated 2-phenylquinoline) iridium(III) complexes demonstrated the strongest ECL.